Chemokine signaling mechanisms underlying inflammation and infection control: Insights from the zebrafish model

Sommer, F.

3 Disruption of Cxcr3 chemotactic signaling alters lysosomal function and renders macrophages more microbicidal

Frida Sommer, Vincenzo Torraca, Eveline in' t Veld, Joost Willemse, Annemarie H. Meijer

Abstract

Chemotaxis and lysosomal function are closely intertwined processes essential for the inflammatory response and clearance of intracellular bacteria. We used the zebrafish model to examine the link between chemotactic signaling and lysosome physiology in macrophages during mycobacterial infection and wound-induced inflammation *in vivo*. Macrophages from zebrafish larvae mutated in a Cxcr3 family chemokine receptor display upregulated expression of vesicle trafficking and lysosomal genes and possess enlarged, highly acidic lysosomes that enhance intracellular bacterial clearance. This increased microbicidal capacity could be phenocopied by blocking the lysosomal Transcription Factor EC, while its overexpression counteracted the protective effect of chemokine receptor mutation. Tracking macrophage migration in zebrafish revealed that lysosomes of chemokine receptor mutants accumulate in the front half of the cell, preventing macrophages to polarize during chemotaxis and reach sites of inflammation. Our work shows that chemotactic signaling affects lysosomal properties and localization during chemotaxis, key aspects of the inflammatory response.

Introduction

Leukocytes differentially express chemokine receptors to sense chemotactic cues that direct them to inflammatory sites [1, 2]. Following chemotactic stimulation, leukocytes acquire a polarized phenotype characterized by clearly identifiable lamellipodia (leading edge) and a uropod (rear edge) that involves both the contractile machinery of the cell and the intracellular vesicle trafficking system [3]. Lysosomes are closely related to cell motility due to their role in lipid catabolism and vesicle trafficking during chemotaxis. The Ca^{2+} release triggered by chemokine receptors induces the fusion of lysosomes with the plasma membrane at the uropod to sustain cell shape remodeling through the delivery of endomembranes and to detach the uropod during chemotaxis [4, 3, 5, 6, 7]. Synaptotagmins (calcium-sensing vesicle-fusion proteins) and Rab GTPases are critical regulators of vesicular trafficking and lysosomal exocytosis and link the chemokine signaling-dependent Ca^{2+} flux to lysosomal function [4, 8, 9]. Processes associating cell motility and lysosomal function are only partially understood and the effect of chemokine signaling on lysosomal function during inflammatory processes *in vivo* remains largely unknown.

Lysosomes are the primary degradative organelles and critical regulators of cell metabolism, and survival [10, 11]. The mammalian/mechanistic target of rapamycin complex 1 (mTORC1), a kinase complex anchored to the lysosomal membrane, is one of the main regulators of lysosomal function [12, 13]. The serine/threonine kinase mTOR phosphorylates the master gene of lysosomal biogenesis TFEB (transcription factor TB) to prevent its translocation to the nucleus [14, 15, 16]. TFEB is a member of the basic helix-loop-helix leucine zipper family of transcription factors that bind to the CLEAR (Coordinated Lysosomal Expression and Regulation) elements (GTCACGTGAC) in the promoter regions of autophagic and lysosomal genes [14, 15]. It belongs to the microphthalmia-associated transcription factor and TFE (MiTF/TFE) that also includes TFEC (transcription factor EC), TFE3 (transcription factor E3) and MITF (Melanocyte inducing transcription factor), which are also under mTORC1 regulation [14, 16, 17]. TFE3 homodimers or TFE3-TFEB heterodimers cooperatively orchestrate lysosomal biogenesis and exocytosis by binding to an overlapping set of CLEAR elements [18, 19]. The role of TFEC in development is well known but its involvement in lysosomal function remains poorly understood [20, 21]. Early reports suggest that TFEC acts as a repressor of lysosomal biogenesis [22, 23]. It was later suggested that different isoforms of TFEC can enhance lysosomal biogenesis in a cell-specific manner, and therefore TFEC is now ascribed mostly a dual role [24, 25]. Lysosomes carry out multiple cell-specific tasks [26, 27]. In macrophages and other phagocytic cells, lysosomes are involved in pro-inflammatory, chemoattractant, and antimicrobial responses [5, 26, 28, 29]. Macrophage recognition of pathogen- and damage'associated molecular patterns (PAMPs and DAMPs) activates and primes lysosomes for pathogen degradation and chemotaxis in a mTORC1-independent manner [5, 30, 31]. Macrophages activated by TLR (Toll-like receptor) sensing of live bacteria or LPS (lipopolysaccharide) show accumulation of TFE3 in the nucleus and the induction of immune genes directly implicated in the inflammatory response [28, 32]. Likewise, the activation of TFEB leads to increased phagosomal acidification and a significant increase in the total number of lysosomes [28, 31, 27]. By contrast, depletion of TFEB or TFE3 results in dampening of cytokine and chemokine secretion [28, 29, 27]. Thus, the function of the lysosomal transcriptional regulators is tightly linked to the production of chemotactic signals directing macrophage migration.

Pathogen sensing through TLRs triggers the release of intracellular calcium from the lysosome through the MCOLIN 1 (mucolipin 1) ion-channel and activates calcineurin, which dephosphorylates TFEB and facilitates its translocation to the nucleus independently of mTORC1 [5, 33, 34, 32]. Induction of microbicidal genes also occurs independently of mTORC1 upon overexpression of the master metabolic modulator 5'AMPK (activated protein kinase) and depletion of its negative regulator FLCN (folliculin), which acts upstream of TFEB/TFE3 [31]. An additional mTORC1-independent mechanism involves the Rag-Ragulator complex in microglia [30, 35]. The Rag-Ragu-

lator complex refers to heterodimeric complexes of RagA or RagB GTPases coupled to either RagC or RagD [36, 37, 38]. These complexes anchor TFEB/TFE3 to the lysosomal membrane and control the intracellular distribution of the transcription factors [37, 39, 40]. In a study using zebrafish, RNA sequencing analyses showed upregulation of multiple lysosomal genes in microglia of RagA (*rraga*) mutant zebrafish larvae [30].

In the present study, we investigated the link between chemotactic signaling and lysosomal function *in vivo* using a *cxcr3.2* mutant zebrafish line which is deficient in a macrophage-attractant chemokine receptor homologous to human CXCR3 [41]. We previously showed that zebrafish larvae lacking this chemokine receptor have increased resistance towards mycobacterial infection and their macrophages show reduced motility and a rounded shape [41, 42]. Here we report that RNAseq data of these macrophages revealed a dysregulation of lysosomal and Golgi- related genes. In agreement, we found that the disruption of chemokine signaling in these cells was linked to increased lysosomal contents. Disruption of the Cxcr3 axis resulted in enhanced clearance of ingested material, specifically a mycobacterial pathogen. Supporting the connection between Cxcr3 chemotactic signaling and lysosomal function, we found that blocking Tfec phenocopied the infection resistance of chemokine receptor mutants, while their enhanced microbicidal capacity was counteracted by increasing *tfec* levels. Finally, we assessed if the aberrant macrophage motility in the chemokine receptor mutants was linked to altered subcellular dynamics of lysosomes during cell migration. Indeed, we observed that cell polarization in mutant macrophages was incomplete, with lysosomes largely failing to shuttle between the leading and trailing edges of the cell. Taken together, these results link macrophage chemotaxis to intracellular vesicular trafficking, showing that disruption of the Cxcr3 axis leads to the induction of lysosomal gene expression and enhanced microbicidal capacity, which primes macrophages for defense against intracellular bacteria.

Materials and Methods

Zebrafish lines and husbandry

Zebrafish were handled in compliance with guidelines from the Zebrafish Model Organism Database (http://zfin.org), the EU Animal Protection Directive 2010/63/EU, and the directives of the local animal welfare committee of Leiden University (License number: 10612). The wt fishline used in this study is AB/TL. The homozygous mutant (*cxcr3.2-/-*) and homozygous wildtype (wt) siblings (*cxcr3.2+/+*) of the *cxcr3.2*^{hu6044} allele were crossed into the Tg (*mpeg1:mCherry-F*)^{ump2} background to visualize macrophages. Zebrafish larvae and eggs were stored at 28.5°C in egg water (60 µg/ml Instant Ocean sea salts and 0.0025% methylene blue) and anesthetized with 0.02% buffered tricaine, (3-aminobenzoic acid ethyl ester; Sigma Aldrich, St. Louis, MO, USA) before infections

and imaging. Larvae were kept in E2 medium (15 mM NaCl; 0.5 mM KCl, 1.0 mM $MgSO_4$, 150 μM KH_2PO_4, 50 μM Na_2HPO_4, 1mM $CaCl_2$; 0.7 mM $NaHCO_3$) for a minimum of 6h prior and during experimental procedures involving pH-rodo and LysoTracker. For confocal imaging, larvae were kept in egg water containing 0.003% PTU (1-phenyl-2-thiourea, Sigma Aldrich) to prevent pigmentation.

FACS, RNA extraction and cDNA synthesis

For RNA sequencing experiments, three biological samples of 150-200 6dpf Tg *(mpeg1:mCherry-F cxcr3.2-/- and cxcr3.2+/+)* larvae were dissociated for FACS following the procedure described in [43]. For qPCR analysis on sorted cells, three biological samples of 100-200 Tg *(mpeg1:mCherry-F cxcr3.2-/- and cxcr3.2+/+)* 5dpf larvae were used. For both procedures, RNA was extracted using the miRNeasy mini kit (Qiagen) according to the manufacturers' instructions. For RNA sequencing, the synthesis of cDNA was done using the SMARTer® Universal Low Input RNA Kit for Sequencing (Clontech) following the manufacturer's guidelines.— For qPCR analysis, cDNA was generated using the iScript™ cDNA Synthesis Kit (Bio-Rad).

RNA-sequencing analysis

Illumina RNA sequencing, mapping and counting of reads was performed as described previously [43]. RNA sequencing data analysis was done with the DESeq2 bioinformatics package (https://bioconductor.org/packages/release/bioc/html/DESeq2 .html) [44]. Before data processing, lowly expressed genes (<50 total reads) were filtered. Genes with a p.adj < 0.05 and $|\log2(\text{fold change})| > 0.5$ cut off were selected for gene ontology analyses (**Supplementary Dataset 1**). Correspondence between human and zebrafish orthologs was derived through g:profiler (http://biit.cs.ut.ee/gprofiler) and manually curated [47] (**Supplementary Table 1**). The significantly affected KEGG pathways were determined by submitting the predicted human orthologs of the significantly regulated zebrafish genes to DAVID bioinformatics tools (david. ncifcrf.gov) [45, 46] (**Supplementary Dataset 2**). The significantly affected Gene Ontology (GO) terms were determined by submitting the predicted human orthologs of the significantly regulated zebrafish genes to PANTHER (geneontology.org). Gene enrichment analysis criteria were Fisher Exact test or False Discovery Rare (FDR) < 0.05 (for DAVID or PANTHER respectively), number of affected genes ≥ 10, fold enrichment ≥ 1.5. Raw data are deposited in the Gene Expression Omnibus database under accession number GSE149942. The complete data analysis (**Supplementary Datasets1-3**) are available following the link: **https://doi.org/10.5281/zenodo.3833848**

Quantitative PCR analysis

For qPCR analyses on *cxcr3.2* expression, three batches of 10 ABT/TL larvae injected with DN-*tfec*, *CMV:tfec* or PBS each, were collected in QIAzol lysis reagent (Qiagen). Similarly, 3 batches of infected and non-infected AB/TL larvae were collected to assess

tfec induction upon infection. Reactions were run on a MyiQ Single-Color Real-Time PCR Detection System (Bio-Rad) using iTaq™ Universal SYBR® Green Supermix (Bio-Rad). Three technical replicates were done for every biological sample. The cycling conditions were: 3 min pre- denaturation at 95°C, 40 denaturation cycles for 15 sec at 95°C, annealing for 30 sec at 60°C (for all primers), and elongation for 30 sec at 72°C. We used the housekeeping gene *ppiab* (peptidylprolyl isomerase Ab) for whole larvae, and *eif5* for sorted macrophages and analyzed the data with the 2 –ΔΔCt method**.** Primer sequences can be found in **Supplementary Table 1.** A One-way ANOVA was used to test for significance of the sorted macrophages data and results are plotted as mean ± SEM (ns p> 0.05, * p ≤ 0.05, **p ≤ 0.01, *** p ≤ 0.001). For *cxcr3.2* expression and *tfec* induction on whole larvae, we used a two-tailed T-test and plotted the results as mean ± SEM (ns p> 0.05, * p ≤ 0.05, **p ≤ 0.01, *** p ≤ 0.001).

Assessment of microbicidal capacity

To determine the microbicidal capacity of zebrafish larval macrophages, embryos were infected with 200 CFU of the attenuated strain, *ΔERP-M. marinum-mWasabi*. Larvae were infected in the blood island (BI) with 1nL of a *ΔERP-M. marinum-mWasabi* single-use glycerol stock and microinjected at 28hpf. Infected larvae were fixed with 4% paraformaldehyde (PFA) at 44 hpi, mounted in 1.5% low-melting-point agarose (SphaeroQ, Burgos, Spain) and bacterial clusters were quantified under a Zeiss Observer 6.5.32 laser scanning confocal microscope (Carl Zeiss, Sliedrecht, The Netherlands) using a CApochromat 63x/1.20 W Corr UV-VIR-IR objective (Carl Zeiss). We used a Mann-Whitney test to analyze the overall bacterial burden of the pooled data of 2 independent replicates of 12-15 fish each, where data are shown as mean ± SEM. A Kolmogorov-Smirnov test was used to analyze the distribution of bacterial cluster sizes (ns p>0.05, * p≤0.05, **p ≤ 0.01, *** p ≤ 0.001, **** p ≤ 0.0001).

Acidification assessment using pH-rodo

cxcr3.2 mutant and wt larvae were injected with 1 nL of *E. coli* pH-rodo bioparticles conjugate for phagocytosis (Invitrogen) at 28-37 hpf into the BI and imaged over the circulation valley at 30-45 minutes post-injection (mpi). In all cases, the same area was imaged by mounting anesthetized larvae in 1.5% low-melting-point agarose and imaged with Plan-Neofluar 40x/0.9 Imm corr objective on a Zeiss Observer 6.5.32 laser-scanning confocal microscope (Carl Zeiss, Sliedrecht, The Netherlands). Fluorescence intensity was assessed using FIJI/ Image J quantification tools and data were analyzed using a two-tailed T-test. Results are shown as mean ± SEM (ns p> 0.05, * p≤0.05, **p ≤ 0.01, *** p ≤ 0.001, **** p ≤ 0.0001). Results are expressed as % relative to the wt control (100%).

LysoTracker staining of acidic compartments

2-day-old *cxcr3.2* mutant and wt larvae were incubated for 1-2 h with 10μM LysoTrack-

er green DND-26 (Invitrogen) in E2 medium. Larvae were anesthetized following the staining and rinsed 3 times for 5 min each with E2 medium and tricaine. Images of live macrophages were acquired with a Plan-Neofluar 40x/0.9 Imm corr objective on a Zeiss Observer 6.5.32 laser-scanning confocal microscope (Carl Zeiss, Sliedrecht, The Netherlands). To quantify LysoTracker staining within macrophages, the mean intensity of LysoTracker overlapping with *mpeg1:mCherry* signal was measured using FIJI/Image J quantification tools. Data were analyzed using a two-tailed t-test. Results are shownas mean ± SEM (ns p> 0.05, * p≤0.05, **p ≤ 0.01, *** p ≤ 0.001, **** p ≤ 0.0001). Results are expressed as % relative to the wt control (100%).

Systemic infection with *Mycobacterium marinum* and determination of bacterial burden

M. marinum M-strain expressing the fluorescent marker mCherry was grown and prepared freshly for injection as described in [48]. Embryos were systemically infected with 300CFU of *M. marinum*-mCherry by microinjection in the BI at 28hpf. Infected larvae were imaged under a Leica M165C stereo-florescence microscope at 4 days post-infection, and the bacterial burden was determined using a dedicated pixel counting program [49]. Data were analyzed using a two-tailed t-test. Results are shown as mean ± SEM (ns p> 0.05, * p≤0.05, **p ≤ 0.01, *** p ≤ 0.001, **** p ≤ 0.0001) and combined data of 3 independent replicates of 20-30 larvae each.

Transient *tfec* overexpression and Tfec function blockade

An expression construct pcDNA™3.1/V5-His TOPO-*CMV:tfec* was injected into the yolk at 0 hpf to overexpress the gene in wt and *cxcr3.2* mutant larvae. Overexpression levels were verified by qPCR analysis. Tfec function was blocked by injecting a DN-*tfec* construct in wt larvae at 0 hpf. Tfec function blockade was verified through qPCR on *kitlgb*, a downstream target of Tfec [20].

Lysosome localization within migrating macrophages

Time-lapse images of LysoTracker stained macrophages of 3-day-old *cxcr3.2* mutant and wt larvae (5 larvae per genotype) were acquired 1 after tail-amputation every 30 sec for 1h. Larvae were mounted in 1.5 % low-melting-point agarose and microscopy was done using a Leica TCS SP8 MP confocal microscope (Leica Microsystems). Data were analyzed using a Fiji/ImageJ homemade plugin "Lysosomal distribution" (**https://sites.imagej.net/Willemsejj/**). The plugin divides the total area of single macrophages in half and quantifies the proportion of LysoTracker staining in each part of the cell in every time-frame (**Supplementary File 1**). The data were organized by cell and by fish and analyzed with a two-tailed t-test a Mann-Whitney test, respectively. Data are shown as mean ± SEM (ns p > 0.05, * p ≤ 0.05, **p ≤ 0.01, *** p ≤ 0.001, **** p ≤ 0.0001).

Results

Intracellular vesicle trafficking and lysosomal genes are upregulated when the Cxcr3.2 chemotactic signaling is disrupted

The zebrafish Cxcr3.2 chemokine receptor is a functional homolog of human CXCR3. Macrophages lacking this receptor have impaired motility and a rounded shape compared to their wildtype (wt) counterparts [41, 42]. To identify the genes and biological pathways affected by the disruption of Cxcr3 signaling, we isolated macrophages from *cxcr3.2* mutant and wt zebrafish larvae and subjected these to RNA deep sequencing (RNAseq). Principal component analysis (PCA) confirmed overall distinction between the *cxcr3.2* mutant and wt transcriptomic profiles (**Figure 1A**). Differential expression analysis revealed that *cxcr3.2* mutation leads to the downregulation of 490 genes and upregulation of 407 genes (**Supplementary Dataset 1**) and genes related to different subcellular compartments (**Figure 1B, Supplementary Dataset 2**). Classification of these genes by compartment showed that peroxisomal, lysosomal and Golgi-related genes were most frequently up-regulated (**Figure 1C, Supplementary Dataset 2**), although only lysosomal and Golgi related terms were significantly differentially represented in GO or KEGG enrichment analysis, *i.e.* KEGG 'Lysosome', GO Cellular components 'Golgi-associated vesicle', 'Golgi apparatus', 'ER-Golgi intermediate compartment', 'Lysosome', 'Vacuole' and GO Biological process 'Golgi vesicle transport' (**Supplementary Dataset 3**). Differentially expressed genes related to lysosomal and Golgi function could also be classified under different processes, including Golgi stacking, post-Golgi coating, Endoplasmic reticulum (ER) to Golgi trafficking, Golgi post-translational modifications (Golgi-PTM), Endosome-lysosome trafficking, Trans Golgi network (TGN) function, lysosomal biogenesis and maturation, and proton transport (**Figure 1D**). To confirm the upregulation of genes involved in lysosomal function, we ran a qPCR on lysosomal markers *ctsl.1* (lysosomal cysteine protease), *atp6v1c1b* (acidifies intracellular compartments) and *slc36a1* (lysosomal amino acid transporter) and the lysosomal regulators *tfeb*, *tfe3,* and *tfec*. All lysosomal markers showed upregulation comparable to those observed in the RNAseq profile (**Figure 1E,F**). However, the expression of the lysosomal regulatory genes was unaffected, indicating that the effects on lysosomal gene expression cannot be attributed to changes in the transcription of *tfeb*, *tfe3b* or *tfec*. Altogether, our data suggest that disruption of the zebrafish Cxcr3 axis induces a transcriptional increase in genes related to lysosomal function and intracellular vesicle trafficking, independently of expression changes in the lysosomal biogenesis regulators *tfeb*, *tfe3b*, and *tfec*.

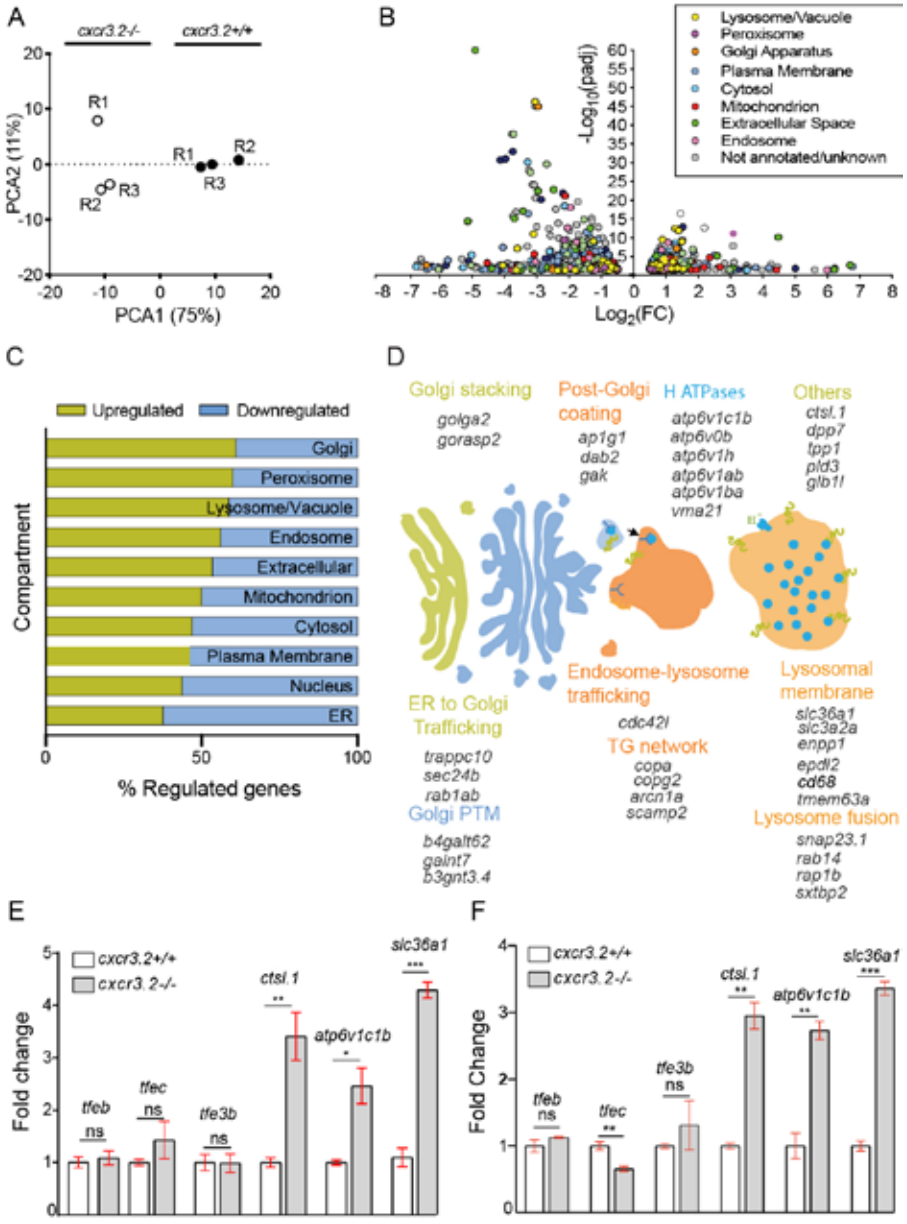

Figure 1. Disruption of Cxcr3.2 signaling transcriptionally induces genes related to lysosomal function and intracellular vesicle trafficking. Principal component analysis (PCA) of *cxcr3.2* mutant and wt transcriptomes. PCA analysis was performed in R on variance-stabilizing transformed (vst) data, using the Deseq2 'plotPCA' command (**A**). Volcano plot of *cxcr3.2* mutant versus wild type differentially expressed genes. Genes are classified and color-coded by cellular compartment annotation. Compartment annotations were obtained from genontology.org according to GO: Cellular component and from KEGG pathways (**B**). Distribution of upregulated (yellow) and downregulated

(blue) genes, classified by compartment as above Lysosomal, Golgi and peroxisome-related genes are more commonly upregulated in *cxcr3.2* mutant macrophages (**C**). Graphical representation of induced genes exerting key functions in Golgi and Lysosomal pathways (**D**). Expression fold change of representative lysosomal markers and transcriptional regulators of lysosomal functions of *cxcr3.2* mutant wt FACS-sorted macrophages, as determined by qPCR (**E**) or RNAseq analysis (**F**). qPCR analysis confirmed that overall lysosomal function is increased in *cxcr3.2* mutants as indicated by the upregulation of lysosomal function markers ctsl.1, atp6v1c1b, and slc36a1, whereas the expression of the lysosomal biogenesis regulators *tfeb*, *tfe3* and *tfec* remained unaltered.These data were analyzed using a two-tailed t-test and results are shown as mean ± SEM (ns $p>0.05$, * $p\leq0.05$, ** $p \leq 0.01$, *** $p \leq 0.001$). *Figure 1B-D wASmodified from Torraca, 2016.

Disruption of chemotactic signaling increases the lysosomal content and microbicidal capacity of macrophages

To assess whether altered expression of vesicle trafficking and lysosomal genes impacts the lysosomal function we investigated the microbicidal capacity of macrophages in *cxcr3.2* mutant and wt embryos. We had previously shown that *cxcr3.2* mutation increases overall resistance of zebrafish embryos to *M. marinum*, a mycobacterial pathogen that is widely used to model tuberculosis infection [41, 50, 51]. However, our previous work did not address the competency of individual macrophages in eliminating the mycobacterial infection. Therefore, we infected *cxcr3.2* mutant and wt embryos with the *ΔERP* mutant *M. marinum* strain. This strain lacks the *ERP* (exported repetitive protein) virulence factor that confers resistance to acidity and allows mycobacteria to replicate inside phagolysosomes. As demonstrated in previous studies, clearance of *ΔERP* mutant *M. marinum* by macrophages serves as an indicator of microbicidal efficacy because one can track the clearance of a stationary bacterial population [52]. Our data show that *cxcr3.2* mutant embryos were more efficient at clearing the infection than the wt controls because they developed fewer and smaller bacterial clusters (**Figure 2A-B**). To assess if enhanced clearance of bacteria in *cxcr3.2* mutants was related to a higher phagolysosome and lysosome acidity, we injected pH-rodo *E.coli* bioparticles into the circulation valley of 3 dpf wt and *cxcr3.2* mutant larvae. The pH-rodo *E.coli* bioparticles fluoresce at low pH values and the fluorescence intensity increases with acidity. In line with the RNA sequencing data and the augmented microbicidal efficacy, phagosomes from *cxcr3.2* mutant macrophages were more acidic at 30-40 minutes post-injection (mpi) than macrophages in wt larvae (**Figure 2C-E**). We then assessed whether the upregulation of lysosomal genes had an effect on the size and number of lysosomal vesicles within macrophages. We bath-exposed 2dpf wt and *cxcr3.2* mutant embryos to the intravital LysoTracker dye and proceeded to quantify the area of the staining within single macrophages. Lysosomal contents were more abundant in *cxcr3.2* mutants than in wt controls (**Figure 2F-H**). These *in vivo* experiments support that the upregulation of lysosomal genes in *cxcr3.2* mutants affects both the properties and the number of lysosomal vesicles and acidic compartments, thereby rendering macrophages with a disrupted Cxcr3 chemokine signaling axis more microbicidal than their wt counterparts.

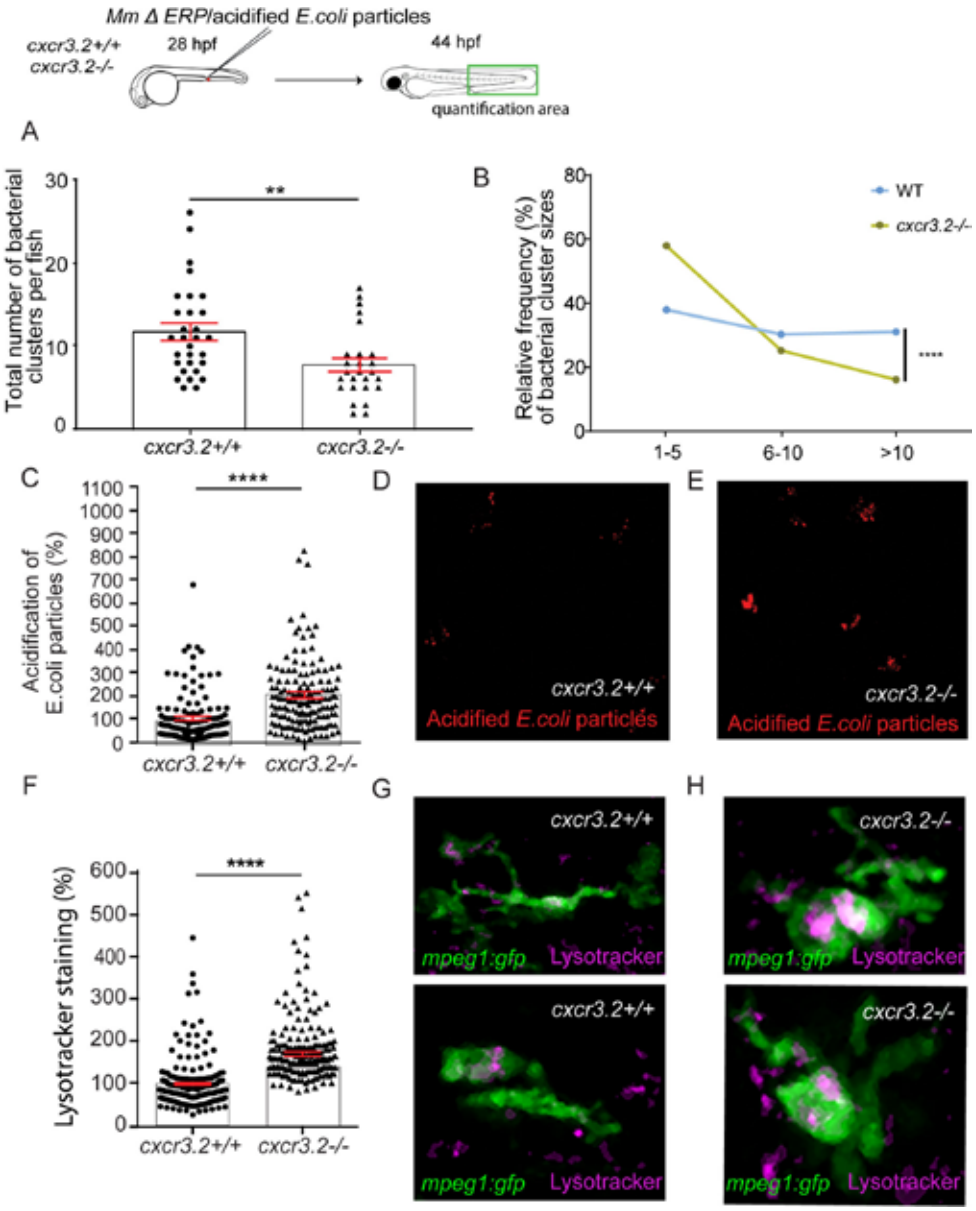

Figure 2. The upregulation of lysosomal genes in *cxcr3.2* mutants is associated with increased microbicidal activity of macrophages. We systemically infected *cxcr3.2* mutant zebrafish embryos and their wt siblings with the attenuated *M. marinum* Δ*ERP wasabi* strain. Quantification of bacterial clusters at 44 hpi in the indicated area showed that infected *cxcr3.2* mutants develop fewer bacterial clusters than their wt siblings (**A**). Furthermore, *cxcr3.2* mutants have a higher frequency of smaller bacterial clusters (1-5 bacteria) and a lower frequency of larger cluster (>10 bacteria) than wt controls (**B**). The normalized intensity (%) of pH-rodo *E.Coli* bioparticle clusters in *cxcr3.2* mutants is

higher than in wt larvae based on fluorescence quantification and representative images (**C-E**). Normalized data of LysoTracker staining show that *cxcr3.2* mutant macrophages have higher lysosomal contents (%) than wt controls based on fluorescence quantification and representative images (2 per genotype) (**F-H**). A Mann-Whitney test was conducted to analyze the total number of bacterial clusters per fish of the pooled data of 2 independent replicates of 12-15 fish each (**A, C**, and **F**) and a Kolmogorov-Smirnov test was used to analyze the distribution of bacterial cluster sizes (**B**). All data are shown as mean ± SEM (**p ≤ 0.01, **** p ≤ 0.0001). Scale bars: 5µm * Figure 2A-F were modified from Torraca, 2016.

Blocking Tfec function phenocopies the increased resistance of *cxcr3.2* mutants to mycobacterial infection

Having linked the *cxcr3.2* mutant phenotype to increased lysosomal contents and enhanced bacterial clearing, we asked whether this phenotype could be evoked by manipulating one of the lysosomal regulators. We chose Transcription factor EC (Tfec) for this purpose because well-characterized molecular tools are available to modulate its function [20]. Tfec isoforms can act either as lysosomal biogenesis repressors or transactivators depending on the cell type that expresses them [24, 25]. Tfec can form heterodimers with Tfe3 which together with the lysosomal biogenesis master gene, Tfeb, coordinates lysosomal biogenesis and function [53, 54]. To assess the predominant role of Tfec on lysosomal function and the innate immune response, we injected a dominant-negative construct (DN-*tfec*) into the yolk of wt embryos at 0 hpf and subsequently infected them with *M. marinum*. Blocking Tfec function (**Supplementary Figure 1B**) resulted in a lower bacterial burden at 4 dpi (**Figure 3A-B**). By contrast, when *tfec* was overexpressed by injecting a *CMV:tfec* construct (**Supplementary Figure 1A**) instead of the dominant-negative construct, larvae had a higher bacterial burden than PBS-injected controls (**Figure 3C-D**). We asked whether *tfec* expression changes upon *M. marinum* infection, but qPCR analyses demonstrated that *M. marinum* infection does not alter *tfec* transcription (**Supplementary Figure 2**). Furthermore, we verified that *tfec* overexpression or Tfec function blockade did not affect expression levels of *cxcr3.2* itself (**Supplementary Figure 3**). Our data show that in the context of innate immunity, *tfec* increases the susceptibility of zebrafish larvae to mycobacterial infection presumably by limiting the clearance of bacteria and that blocking Tfec function phenocopies the increased resistance to *M. marinum* of *cxcr3.2* mutant larvae.

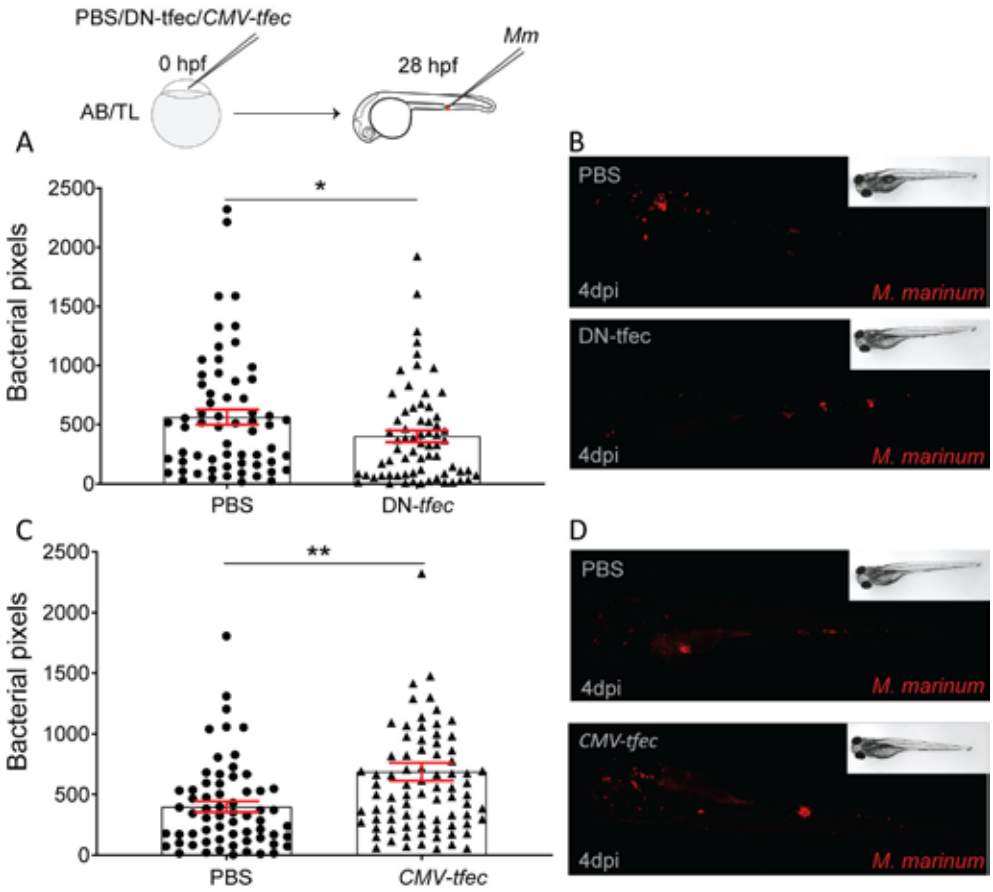

Figure 3. Blocking Tfec function phenocopies the increased resistance of *cxcr3.2* mutants towards *M. marinum* infection. We blocked Tfec function by injecting a dominant-negative construct (DN-*tfec*) (**A-B**) or transiently overexpressed the gene by injecting a *CMV:tfec* construct (**C-D**) in AB/TL eggs at 0 hpf. We subsequently infected the larvae with *M. marinum mCherry* and assessed infection at 4dpi by fluorescent pixel quantification from stereo fluorescence images (representative examples shown). Larvae injected with DN-*tfec* have a lower bacterial burden than PBS injected controls at 4dpi (**A-B**). By contrast, *CMV:tfec* injected larvae have a higher bacterial burden than controls (**C-D**). The bacterial burden data were analyzed using a two-tailed t-test. Results are shown as mean ± SEM (* $p \leq 0.05$, ** $p \leq 0.01$).

Tfec counteracts the enhanced microbicidal capacity of *cxcr3.2* mutants

To confirm if *tfec* alters mycobacterial clearance efficacy by directly affecting the microbicidal capacity of macrophages we used the Δ*ERP* mutant *M. marinum* strain that is sensitive to lysosomal acidification. We blocked Tfec function with the DN-*tfec* construct and observed that larvae developed fewer and smaller bacterial clusters than PBS-inject-

ed controls (**Figure 4A-B**). Next, we transiently overexpressed *tfec* in *cxcr3.2* mutants and confirmed that *tfec* overexpression counteracts the enhanced microbicidal capacity of the *cxcr3.2* mutants towards the *ΔERP* mutant *M. marinum* strain. Tfec overexpression in the *cxcr3.2* mutant background yields an overall bacterial burden comparable to wt controls and larger bacterial clusters, while non-injected mutants preserve their enhanced microbicidal capacity showing a low bacterial burden and fewer large bacterial clusters (**Figure 4C-D**). We conclude that Tfec function counteracts enhanced microbicidal properties of macrophages that arise from disrupting Cxcr3 chemotactic signaling.

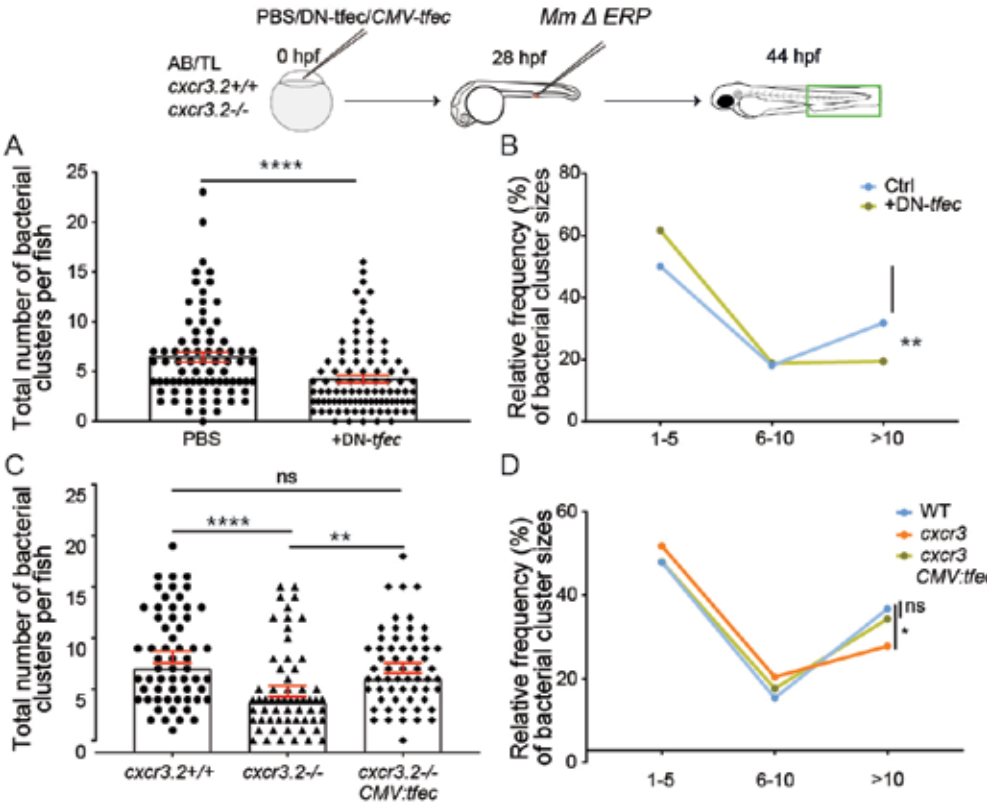

Figure 4. *tfec* overexpression counteracts enhanced microbicidal capacity of *cxcr3.2* mutants. Tfec function was blocked by injecting the DN-*tfec* construct into AB/TL eggs at 0 hpf. Larvae were infected with *the M. marinum ΔERP wasabi* strain. Larvae injected with DN-*tfec* developed fewer and smaller bacterial clusters than PBS injected larvae (**A-B**) and phenocopied *cxcr3.2* mutants in their capacity to clear bacteria (**Figure 2**). Similarly, Tfec was overexpressed by injecting a *CMV:tfec* construct at 0hpf in *cxcr3.2* mutants, prior to infection *with M. marinum ΔERP wasabi*. *CMV:tfec* expressing *cxcr3.2* mutants lose their enhanced microbicidal capacity and have more and larger bacterial clusters than PBS injected mutants, reaching similar levels as the wt controls (**C-D**). The total number of bacterial clusters per fish were analyzed using a Mann-Whitney test and combines the data of 3 independent replicates of 20-30 larvae (**A** and **C**). A Kolmogorov-Smirnov test was used to analyze the distribution

of bacterial cluster sizes between 1-5, 6-10 and >10 bacteria (B and D). All data are shown as mean ± SEM (ns $p>0.05$, * $p\leq0.05$, ** $p \leq 0.01$, *** $p \leq 0.001$ **** $p \leq 0.0001$).

The disruption of chemotactic signaling in *cxcr3.2* mutant macrophages alters lysosome trafficking and prevents cell polarization during chemotaxis

Chemokine signaling ultimately triggers the release of intracellular calcium to orchestrate highly dynamic cell membrane rearrangements that result in a polarized phenotype with a clear distinction between the leading edge (lamellipodia) and the trailing edge [4, 3]. Lysosome exocytosis plays a major role in leukocyte chemotaxis as it delivers layers of lipid membrane to sustain plasma membrane turnover and extension towards chemotactic cues, while also mediating the detachment of the uropod [4, 5, 7]. Therefore, as cells move, lysosomal contents shuttle between the lamellipodia and the uropod but transiently concentrate in the latter [9, 8]. Chemokine receptors are required for the formation of the uropod in the rear end of migrating cells [3]. Since *cxcr3.2* mutant macrophages are less motile than wt we assess the localization of lysosomal contents during chemotaxis as an indicator of cell polarization. We stained 3-day-old Tg (*mpeg1-mCherry*) *cxcr3.2* mutant and wt and larvae with the intravital dye LysoTracker and divided the total macrophage area into halves to calculate the anterior-posterior ratio of LysoTracker staining within the cell (**Supplementary File 1**). Macrophages have recognizable leading and trailing edges and lysosomal contents move continuously from the rear to the front (1.15:1) as cells follow a chemotactic signal in wt larvae (**Figure 5A and C**). By contrast, the leading edge and the uropod of *cxcr3.2* mutant macrophages are not well defined and lysosomal contents accumulate in the anterior half of the cell (1.74:1) close to the center in mutant larvae (**Figure 5B and C**). We observed the same trend when single cells were analyzed. The average anteroposterior LysoTracker staining in wt macrophages is 1.13:1 compared with 1.99:1 in *cxcr3.2* mutants (**Figure 5D**). These data show that macrophages lacking Cxcr3.2 are not properly polarized and that lysosomal vesicle trafficking is disrupted in the absence of the chemokine receptor as lysosomes rarely reach the uropod in the absence of Cxcr3 (**Supplementary Figure 4**). This vesicle trafficking defect leads to the accumulation of lysosomal contents and is tightly linked to aberrant macrophage chemotaxis.

Discussion

Recent studies revealed that leukocyte chemotaxis is inextricably intertwined with the subcellular localization and exocytosis of lysosomes [4, 5, 55, 8, 56]. However, our understanding of the complex network of processes linking chemotaxis and lysosomal function in different contexts is only beginning to be understood. Here, we used the zebrafish model to study the conserved Cxcr3 signaling axis, which mediates proinflammatory responses of multiple leukocytes, implicated in several human inflammatory

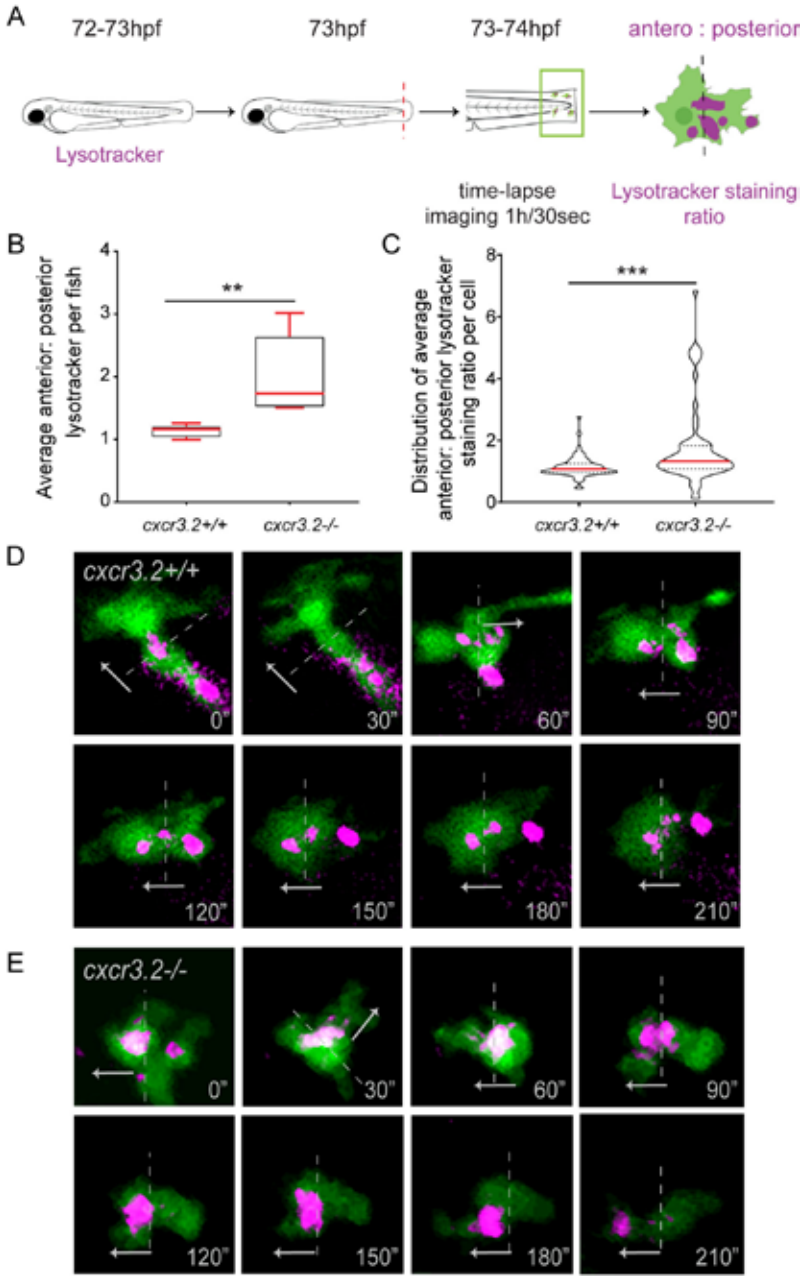

Figure 5. The disruption of Cxcr3.2 signaling in macrophages alters lysosome trafficking and prevents cell polarization during chemotaxis. We assessed the localization of lysosomes during chemotaxis by quantifying the ratio of lysosomal contents in the anterior and posterior halves of migrating macrophages. Tg (*mpeg1-mCherry*) *cxcr3.2* mutant and wt larvae were incubated in LysoTracker and time-lapse images of migrating macrophages after tail-amputation were acquired (**A**). The data shown in **B** and **C** derive from 5 wt and 5 *cxcr3.2* mutant larvae and a total of 63 wt macrophages and 57 mutant macrophages (7≤ cells/fish). The data show the average anterior: posterior LysoTracker

staining ratio per fish (**B**) and the distribution of average staining among cells (**C**). The quantifications and stills at 30sec intervals from representative migration tracks (**D and E**) show that lysosomal contents in wt larvae display a small dispersion in the data (**B and C**) and an even distribution of lysosomes (**D**), while lysosomal contents preferentially accumulate in the anterior half in *cxcr3.2* mutant macrophages (**E**) and show a high variation (**B and C**). The dashed lines indicate the borders between anterior and posterior halves and the arrows indicate the direction in which macrophages move. Data of anterior: posterior LysoTracker staining per fish were analyzed with a Mann-Whitney test and the data per cell were analyzed using a two-tailed t-test. Results are shown as mean ± SEM (**$p \leq 0.01$, ***$p \leq 0.001$). Scale bars: 5μm.

disorders. We show how the disruption of the Cxcr3 chemokine signaling axis in our model leads to transcriptional upregulation of lysosomal genes, increases lysosomal contentsand renders macrophages more microbicidal towards mycobacterial infection despite their altered lysosome trafficking and aberrant motility. These results provide *in vivo* evidence linking lysosomal function to chemotactic signaling that leads us to conclude that disrupting the Cxcr3 chemotactic signaling primes macrophages for better clearance of intracellular infection.

We found a marked dysregulation of lysosomal genes in sorted macrophages of larvae lacking Cxcr3.2, the zebrafish homolog of human CXCR3. In contrast, the expression of lysosomal regulators of the MiTF/TFE protein family remained unaltered, which is in line with previous work showing that members of this protein family are regulated mostly at the posttranscriptional level [23, 25]. The induction of lysosomal genes in *cxcr3.2* mutant macrophages was associated with increased lysosomal contents, higher phagolysosomal acidity, and enhanced clearance of mycobacteria. Previous work by Shen and coworkers used the zebrafish model to assess the lysosomal clearance of apoptotic neuronal debris in RagA (*rraga*) mutant larvae [30]. They reported enlarged lysosomes like in *cxcr3.2* depleted larvae, but a low acidity and poor clearance of apoptotic debris as opposed to our observations in larvae with disrupted chemokine signaling. The RagA GTPase is part of the Rag-Ragulator that anchors TBEB/TFE3 to the lysosomal membrane and interacts with v-ATPases on the lysosomal membrane to acidify the lysosomal lumen [37, 39]. Therefore, the absence of *raga* prevents the anchoring of Tfeb/Tfe3 to the lysosomal membrane and the interaction with v-ATPases, while it promotes the translocation of the transcription factors to the nucleus, arguably leading to a sustained *tfeb*-driven induction of lysosomal genes and a low intraphagosomal acidity [30, 40].

Our results show that the *atp6v1c1b*, and *slc361* genes, that code for the subunit C of the lysosomal v-ATPase (a direct downstream target of Tfeb [14]) and a transmembrane amino acid carrier, respectively, were strongly induced in *cxcr3.2* mutant macrophages together with other lysosomal genes that could be responsible for the highly acidic phagolysosomes in macrophages upon disruption of the Cxcr3 axis. The upregulation of *ctsl.1*, which encodes the endopeptidase Cathepsin L.1 that is involved in catabolic processes and the immune response, could also be linked to the enhanced clearance of bacteria in *cxcr3.2* mutant macrophages.

We observed that blocking the function of Tfec in wt larvae had the same host-protective effect as the *cxcr3.2* mutation upon mycobacterial infection and that *tfec* overexpression resulted in poor control of bacterial dissemination (**Figure 3**). Furthermore, *tfec* overexpression in *cxcr3.2* mutants reverted the protective effect of the mutation and the enhanced clearance of intracellular bacteria (**Figure 4**). Unlike the remaining members of the MiTF/TFE protein family, Tfec is not ubiquitously expressed and, since a Tfec isoform lacks an acidic domain associated with the transactivating function of the other three transcription factors, it can strongly inhibit the Tfe3-mediated gene transactivation [22, 23, 25]. Based on our observations, we posit that *tfec* antagonizes the *tfe3*-driven transactivation of lysosomal and pro-inflammatory genes and that, therefore, blocking Tfec function leads to enhanced lysosomal function and pathogen resistance. Altogether, these results support that the highly microbicidal phenotype of macrophages with a disrupted Cxcr3 axis is associated with deregulations in lysosomal function.

Lysosomes are major players in a concatenated series of molecular pathways required for chemotaxis in macrophages [4, 57]. As previously shown by our group, *cxcr3.2* mutant macrophages have reduced motility and a rounded shape [41, 42]. Here we showed that Cxcr3.2-depleted macrophages do not show a clear polarized phenotype and that lysosomes localize mainly in the leading edge of the cell and rarely reach the uropod. The disruption of two other chemokine signaling axes, CXCR4/CXCL12 and CCR2/CCL2, was found to result in reduced T-cell migration when synaptotagmin SYT7 and the related protein SYTL5 were downregulated [4]. Synaptotagmins are proteins that sense chemoattractant-induced Ca^{2+} to control lysosomal exocytosis and to release the uropod during chemotaxis. Taking these observations as a precedent, the disruption of the Cxcr3 axis in our study might affect the intracellular levels and distribution of intracellular chemokine receptor-induced Ca^{2+}, leading to ER stress and the observed accumulation of lysosomal contents due to calcineurin-independent Tfeb translocation to the nucleus [53, 58]. Moreover, vesicle trafficking and lysosome exocytosis might be compromised at low intracellular Ca^{2+} concentrations further contributing to the accumulation of lysosomes in *cxcr3.2* mutant macrophages and the resulting aberrant motility of these cells.

The identity of a cell is the major determinant of the functional specificity of a chemokine receptor-ligand interaction [59]. Cells are exposed to multiple extracellular signals that are processed simultaneously. In the context of inflammation, macrophages are exposed to both chemotactic signaling and pathogen- and damage-driven signaling, like TLR-sensing, which also triggers the release of intracellular Ca^{2+} from the lysosome, ER and Golgi apparatus [28, 30, 29]. TLR-signaling activates calcineurin which in turn dephosphorylates TFE3 that induces pro-inflammatory cytokines and potentially primes lysosomes for pathogen clearance [28]. Therefore, the reduced chemotaxis but increased pathogen resistance of *cxcr3.2* mutant macrophages might reflect that extracellular cues

were integrated in such a way that the intracellular pathway aimed at killing pathogens overpowered the one guiding the cell towards inflammatory stimuli, thereby priming macrophages for a better defense against pathogens.

Our results support that disturbances in the Cxcr3-dependent chemokine signaling network affect intracellular vesicle trafficking and lysosome exocytosis of macrophages, thereby preventing them from acquiring a polarized phenotype and to migrate towards inflammatory foci whilst rendering them more microbicidal. Our work contributes to further our understanding of chemotaxis as a complex process that incorporates various physiological processes and integrates different extracellular cues. It emphasizes the importance of vesicle trafficking during chemotaxis and the relevance of transcriptional and posttranscriptional regulation of lysosome function in immunity. The power of the zebrafish model for intravital imaging enabled us to show that there is a direct link between chemokine signaling and lysosomal function that affects both the microbicidal properties and the motility of macrophages.

Acknowledgments
The authors thank Georges Lutfalla (University of Montpellier) for the macrophage-specific zebrafish reporter lines and Christopher Mahony (University of Birmingham) for the DN-*tfec* construct, Yufei Xie and Michiel van der Vaart for advice on time lapse imaging, and all members of the fish facility team for zebrafish care.

Supplementary materials

Supplementary Table 1. Primer used for the qPCR analysis.

Primer	Forward	Reverse
eif5	CAAGTTTGTGCTGTGTCCCG	AGCCTTGCAGGAGTTTCCAA
ppiab	ACACTGAAACACGGAGGCAAAG	CATCCACAACCTTCCCGAACAC
tfeb	GCATTACATGCAGCATCGCATGCC	CGTGTACACATCCAAATGACTGCTGG
tfec	AACAGTACCTCGCTTTGGGC	CAGTGTTCCCAGCTCCTTGA
tfe3b	CTAGGCTCCAACAAAGAGGAGATG	CAAAATGGTTCCCTTGTTCCAGCGC
ctsl.1	CTGGAGGGACAAGGGCTATG3	CTATGGCAACAGATATGGGGCC
atp6v1c1b	GAGTGTGATGCTGTTTGACGGG	CCCACTGGAACCGGGTAATG
slc36a1	GGAGAACGTGTCGTGGCTAA	CTTCAGCGTGGCTATGACTTCCAT

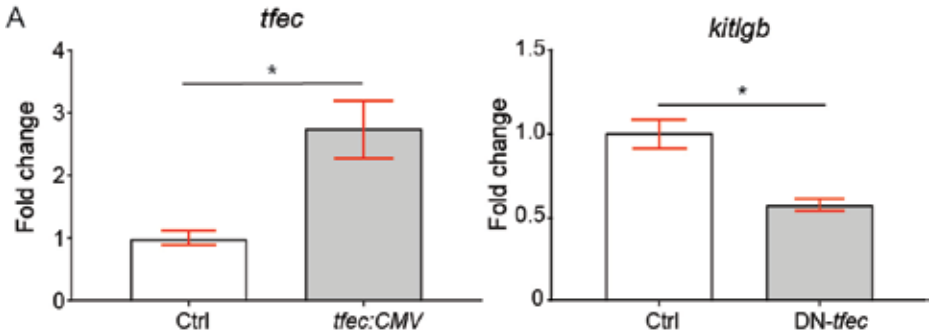

Supplementary Figure 1. qPCR validation of *tfec* overexpression and blockade. qPCR analyses on *CMV:tfec* and DN-*tfec* injected larvae were conducted at 2dpi. Data show that *tfec* was upregulated (n fold=2.65) in *CMV-tfec* injected larvae (**A**). Blocking Tfec function by DN-*tfec* injection results in decreased transcription of the downstream target *kitlgb* . Data were analyzed using a two-tailed t-test and data are shown as mean ± SEM (ns p>0.05, * p≤0.05, **p ≤ 0.01, *** p ≤ 0.001).

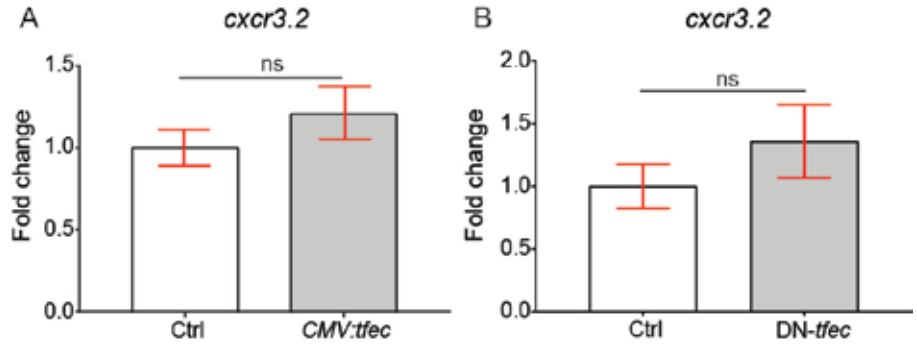

Supplementary Figure 2. Blocking Tfec function or overexpressing *tfec* does not affect the transcription of *cxcr3.2*. Expression of *cxcr3.2* is not transcriptionally affected by Tfec overexpression (**A**) or *tfec* function blockade (**B**). AB/TL larvae were injected with either *DN-tfec*, *CMV:tfec*, or PBS in the yolk at 0 hpf. *cxcr3.2* expression was analyzed through quantitative PCR. Data were analyzed using a two-tailed t-test. Results are shown as mean ± SEM (ns P>0.05).

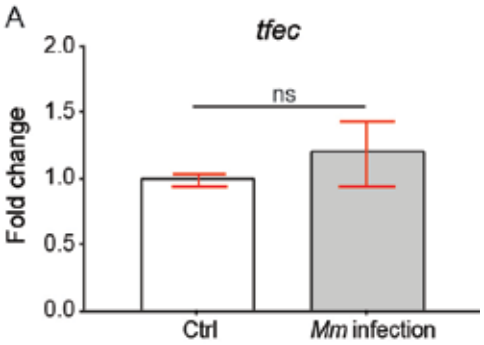

Supplementary Figure 3. *tfec* is not induced upon *M. marinum* infection. AB/TL larvae were systemically infected with *M. marinum* and samples were collected at 2dpi. qPCR analysis of *tfec* indicated no difference between infected larvae and controls. The data were analyzed using a two-tailed t-test and data are shown as mean ± SEM (ns $p>0.05$, * $p\leq0.05$, ** $p \leq 0.01$, *** $p \leq 0.001$).

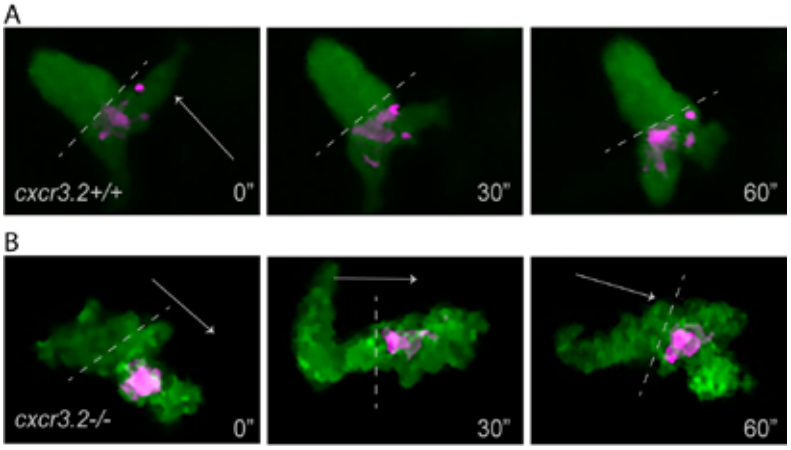

Supplementary Figure 4. Lysosomal contents are rarely found in the uropod of *cxcr3.2* mutant macrophages. During chemotaxis, a clear leading edge and uropod can be recognized in wt macrophages and lysosomes localize in the trailing edge to detach the uropod during cell migration (**A**). Lysosomal contents in *cxcr3.2* mutants generally remain confined to the leading edge and the middle of migrating macrophages and are rarely found in the uropod (**B**). Images are stills at 30sec intervals from representative migration tracks. The dashed lines indicate the borders between anterior and posterior halves and the arrows indicate the direction in which macrophages move. Scale bars: 5μm.

https://doi.org/10.5281/zenodo.3833848

Supplementary Dataset 1: Differentially expressed genes in *cxcr3.2* mutant vs wt FACS-sorted macrophages and orthologous correspondences to human genes.

Supplementary Dataset 2: Classification of differentially expressed genes by cell compartment.

Supplementary Dataset 3: KEGG and Gene Ontology enrichment analysis for the differentially expressed genes of *cxcr3.2* mutant vs wt FACS-sorted.

https://sites.imagej.net/Willemsejj/

Supplementary File 1: Java script for "Lysosomal distribution" Fiji/ ImageJ plugin.

References

[1] I. F. Charo and R. M. Ransohoff, "The many roles of chemokines and chemokine receptors in inflammation," New England Journal of Medicine, vol. 354, pp. 610-621, 2006.
[2] A. Rot and U. H. Von Andrian, "Chemokines in innate and adaptive host defense: basic chemokinese grammar for immune cells," Annu. Rev. Immunol., vol. 22, pp. 891-928, 2004.
[3] M. A. Del Pozo, P. Sánchez-Mateos, M. Nieto and F. Sánchez-Madrid, "Chemokines regulate cellular polarization and adhesion receptor redistribution during lymphocyte interaction with endothelium and extracellular matrix. Involvement of cAMP signaling pathway.," The Journal of cell biology, vol. 131, pp. 495-508, 1995.
[4] R. A. Colvin, T. K. Means, T. J. Diefenbach, L. F. Moita, R. P. Friday, S. Sever, G. S. V. Campanella, T. Abrazinski, L. A. Manice, C. Moita and others, "Synaptotagmin-mediated vesicle fusion regulates cell migration," Nature immunology, vol. 11, pp. 495-502, 2010.
[5] M. Bretou, P. J. Sáez, D. Sanséau, M. Maurin, D. Lankar, M. Chabaud, C. Spampanato, O. Malbec, L. Barbier, S. Muallem and others, "Lysosome signaling controls the migration of dendritic cells," Science Immunology, vol. 2, 2017.
[6] E. L. Becker, "Some interrelations of neutrophil chemotaxis, lysosomal enzyme secretion, and phagocytosis as revealed by synthetic peptides.," The American journal of pathology, vol. 85, p. 385, 1976.
[7] A. Reddy, E. V. Caler and N. W. Andrews, "Plasma membrane repair is mediated by Ca2+-regulated exocytosis of lysosomes," Cell, vol. 106, pp. 157-169, 2001.
[8] G. Constantin and C. Laudanna, "Leukocyte chemotaxis: from lysosomes to motility," Nature immunology, vol. 11, pp. 463-464, 2010.
[9] R. A. Colvin and A. D. Luster, "Movement within and movement beyond: Synaptotagmin-mediated vesicle fusion during chemotaxis," Cell adhesion & migration, vol. 5, pp. 56-58, 2011.
[10] C. De Duve, B. Pressman, R. Gianetto, R. Wattiaux and F. Appelmans, "Tissue fractionation studies. 6. Intracellular distribution patterns of enzymes in rat-liver tissue," Biochemical Journal, vol. 60, p. 604, 1955.
[11] J. A. Martina, H. I. Diab, L. Lishu, L. Jeong-A, S. Patange, N. Raben and R. Puertollano, "The nutrient-responsive transcription factor TFE3 promotes autophagy, lysosomal biogenesis, and clearance of cellular debris," Sci. Signal., vol. 7, pp. ra9--ra9, 2014.
[12] J. A. Martina, Y. Chen, M. Gucek and R. Puertollano, "MTORC1 functions as a transcriptional regulator of autophagy by preventing nuclear transport of TFEB," Autophagy, vol. 8, pp. 903-914, 2012.
[13] C. Settembre, R. Zoncu, D. L. Medina, F. Vetrini, S. Erdin, S. Erdin, T. Huynh, M. Ferron, G. Karsenty, M. C. Vellard and others, "A lysosome-to-nucleus signalling

mechanism senses and regulates the lysosome via mTOR and TFEB," The EMBO journal, vol. 31, pp. 1095-1108, 2012.
[14] M. Sardiello, M. Palmieri, A. Ronza, D. L. Medina, M. Valenza, V. A. Gennarino, C. Di Malta, F. Donaudy, V. Embrione, R. S. Polishchuk and others, "A gene network regulating lysosomal biogenesis and function," Science, vol. 325, pp. 473-477, 2009.
[15] M. Palmieri, S. Impey, H. Kang, A. Ronza, C. Pelz, M. Sardiello and A. Ballabio, "Characterization of the CLEAR network reveals an integrated control of cellular clearance pathways," Human molecular genetics, vol. 20, pp. 3852-3866, 2011.
[16] C. Verastegui, C. Bertolotto, K. Bille, P. Abbe, J. P. Ortonne and R. Ballotti, "TFE3, a transcription factor homologous to microphthalmia, is a potential transcriptional activator of tyrosinase and TyrpI genes," Molecular Endocrinology, vol. 14, pp. 449-456, 2000.
[17] N. Pastore, A. Vainshtein, N. J. Herz, T. Huynh, L. Brunetti, T. J. Klisch, M. Mutarelli, P. Annunziata, K. Kinouchi, N. Brunetti-Pierri and others, "Nutrient-sensitive transcription factors TFEB and TFE3 couple autophagy and metabolism to the peripheral clock," The EMBO journal, vol. 38, 2019.
[18] N. Pastore, A. Vainshtein, T. J. Klisch, A. Armani, T. Huynh, N. J. Herz, E. V. Polishchuk, M. Sandri and A. Ballabio, "TFE3 regulates whole-body energy metabolism in cooperation with TFEB," EMBO molecular medicine, vol. 9, pp. 605-621, 2017.
[19] N. Raben and R. Puertollano, "TFEB and TFE3: linking lysosomes to cellular adaptation to stress," Annual review of cell and developmental biology, vol. 32, pp. 255-278, 2016.
[20] C. B. Mahony, R. J. Fish, C. Pasche and J. Y. Bertrand, "tfec controls the hematopoietic stem cell vascular niche during zebrafish embryogenesis," Blood, The Journal of the American Society of Hematology, vol. 128, pp. 1336-1345, 2016.
[21] J. A. Lister, B. M. Lane, A. Nguyen and K. Lunney, "Embryonic expression of zebrafish MiT family genes tfe3b, tfeb, and tfec," Developmental Dynamics, vol. 240, pp. 2529-2538, 2011.
[22] G. U. A. N. G.-Q. U. A. N. Zhao, Q. Zhao, X. Zhou, M. G. Mattei and B. De Crombrugghe, "TFEC, a basic helix-loop-helix protein, forms heterodimers with TFE3 and inhibits TFE3-dependent transcription activation.," Molecular and cellular biology, vol. 13, pp. 4505-4512, 1993.
[23] E. Steingrı́msson, L. Tessarollo, B. Pathak, L. Hou, H. Arnheiter, N. G. Copeland and N. A. Jenkins, "Mitf and Tfe3, two members of the Mitf-Tfe family of bHLH-Zip transcription factors, have important but functionally redundant roles in osteoclast development," Proceedings of the National Academy of Sciences, vol. 99, pp. 4477-4482, 2002.
[24] M.-C. Chung, H.-K. Kim and S. Kawamoto, "TFEC can function as a transcriptional activator of the nonmuscle myosin II heavy chain-A gene in transfected cells," Biochemistry, vol. 40, pp. 8887-8897, 2001.

[25] K.-i. Yasumoto and S. Shibahara, "Molecular cloning of cDNA encoding a human TFEC isoform, a newly identified transcriptional regulator," Biochimica et Biophysica Acta (BBA)-Gene Structure and Expression, vol. 1353, pp. 23-31, 1997.
[26] C. Settembre, A. Fraldi, D. L. Medina and A. Ballabio, "Signals from the lysosome: a control centre for cellular clearance and energy metabolism," Nature reviews Molecular cell biology, vol. 14, pp. 283-296, 2013.
[27] C. Settembre, C. Di Malta, V. A. Polito, M. G. Arencibia, F. Vetrini, S. Erdin, S. U. Erdin, T. Huynh, D. Medina, P. Colella and others, "TFEB links autophagy to lysosomal biogenesis," science, vol. 332, pp. 1429-1433, 2011.
[28] N. Pastore, O. A. Brady, H. I. Diab, J. A. Martina, L. Sun, T. Huynh, J.-A. Lim, H. Zare, N. Raben, A. Ballabio and others, "TFEB and TFE3 cooperate in the regulation of the innate immune response in activated macrophages," Autophagy, vol. 12, pp. 1240-1258, 2016.
[29] O. Visvikis, N. Ihuegbu, S. A. Labed, L. G. Luhachack, A.-M. F. Alves, A. C. Wollenberg, L. M. Stuart, G. D. Stormo and J. E. Irazoqui, "Innate host defense requires TFEB-mediated transcription of cytoprotective and antimicrobial genes," Immunity, vol. 40, pp. 896-909, 2014.
[30] K. Shen, H. Sidik and W. S. Talbot, "The Rag-Ragulator complex regulates lysosome function and phagocytic flux in microglia," Cell reports, vol. 14, pp. 547-559, 2016.
[31] L. El-Houjeiri, E. Possik, T. Vijayaraghavan, M. Paquette, J. A. Martina, J. M. Kazan, E. H. Ma, R. Jones, P. Blanchette, R. Puertollano and others, "The transcription factors TFEB and TFE3 link the FLCN-AMPK signaling axis to innate immune response and pathogen resistance," Cell reports, vol. 26, pp. 3613-3628, 2019.
[32] J. D. Schilling, H. M. Machkovech, L. He, A. Diwan and J. E. Schaffer, "TLR4 activation under lipotoxic conditions leads to synergistic macrophage cell death through a TRIF-dependent pathway," The Journal of Immunology, vol. 190, pp. 1285-1296, 2013.
[33] D. L. Medina, S. Di Paola, I. Peluso, A. Armani, D. De Stefani, R. Venditti, S. Montefusco, A. Scotto-Rosato, C. Prezioso, A. Forrester and others, "Lysosomal calcium signalling regulates autophagy through calcineurin and TFEB," Nature cell biology, vol. 17, pp. 288-299, 2015.
[34] Y. Tong and F. Song, "Intracellular calcium signaling regulates autophagy via calcineurin-mediated TFEB dephosphorylation," Autophagy, vol. 11, pp. 1192-1195, 2015.
[35] Y. C. Kim, H. W. Park, S. Sciarretta, J.-S. Mo, J. L. Jewell, R. C. Russell, X. Wu, J. Sadoshima and K.-L. Guan, "Rag GTPases are cardioprotective by regulating lysosomal function," Nature communications, vol. 5, pp. 1-14, 2014.
[36] T. Sekiguchi, E. Hirose, N. Nakashima, M. Ii and T. Nishimoto, "Novel G proteins, Rag C and Rag D, interact with GTP-binding proteins, Rag A and Rag B," Journal of Biological Chemistry, vol. 276, pp. 7246-7257, 2001.

[37] L. Bar-Peled, L. D. Schweitzer, R. Zoncu and D. M. Sabatini, "Ragulator is a GEF for the rag GTPases that signal amino acid levels to mTORC1," Cell, vol. 150, pp. 1196-1208, 2012.
[38] J. A. Martina and R. Puertollano, "RRAG GTPases link nutrient availability to gene expression, autophagy and lysosomal biogenesis," Autophagy, vol. 9, pp. 928-930, 2013.
[39] R. Zoncu, L. Bar-Peled, A. Efeyan, S. Wang, Y. Sancak and D. M. Sabatini, "mTORC1 senses lysosomal amino acids through an inside-out mechanism that requires the vacuolar H+-ATPase," Science, vol. 334, pp. 678-683, 2011.
[40] J. A. Martina and R. Puertollano, "Rag GTPases mediate amino acid--dependent recruitment of TFEB and MITF to lysosomes," Journal of Cell Biology, vol. 200, pp. 475-491, 2013.
[41] V. Torraca, C. Cui, R. Boland, J.-P. Bebelman, A. M. Sar, M. J. Smit, M. Siderius, H. P. Spaink and A. H. Meijer, "The CXCR3-CXCL11 signaling axis mediates macrophage recruitment and dissemination of mycobacterial infection," Disease models & mechanisms, vol. 8, pp. 253-269, 2015.
[42] F. Sommer, V. Torraca, S. M. Kamel, A. Lombardi and A. H. Meijer, "Frontline Science: Antagonism between regular and atypical Cxcr3 receptors regulates macrophage migration during infection and injury in zebrafish," Journal of leukocyte biology, vol. 107, pp. 185-203, 2020.
[43] J. Rougeot, A. Zakrzewska, Z. Kanwal, H. J. Jansen, H. P. Spaink and A. H. Meijer, "RNA sequencing of FACS-sorted immune cell populations from zebrafish infection models to identify cell specific responses to intracellular pathogens," in Host-Bacteria Interactions, Springer, 2014, pp. 261-274.
[44] M. I. Love, W. Huber and S. Anders, "Moderated estimation of fold change and dispersion for RNA-seq data with DESeq2," Genome biology, vol. 15, p. 550, 2014.
[45] D. W. Huang, B. T. Sherman, Q. Tan, J. Kir, D. Liu, D. Bryant, Y. Guo, R. Stephens, M. W. Baseler, H. C. Lane and others, "DAVID Bioinformatics Resources: expanded annotation database and novel algorithms to better extract biology from large gene lists," Nucleic acids research, vol. 35, pp. W169--W175, 2007.
[46] B. T. Sherman, Q. Tan, J. R. Collins, W. G. Alvord, J. Roayaei, R. Stephens, M. W. Baseler, H. C. Lane, R. A. Lempicki and others, "The DAVID Gene Functional Classification Tool: a novel biological module-centric algorithm to functionally analyze large gene lists," Genome biology, vol. 8, p. R183, 2007.
[47] J. Reimand, T. Arak, P. Adler, L. Kolberg, S. Reisberg, H. Peterson and J. Vilo, "g: Profiler—a web server for functional interpretation of gene lists (2016 update)," Nucleic acids research, vol. 44, pp. W83--W89, 2016.
[48] K. Takaki, J. M. Davis, K. Winglee and L. Ramakrishnan, "Evaluation of the pathogenesis and treatment of Mycobacterium marinum infection in zebrafish," Nature protocols, vol. 8, p. 1114, 2013.

[49] E. J. M. Stoop, T. Schipper, S. K. R. Huber, A. E. Nezhinsky, F. J. Verbeek, S. S. Gurcha, G. S. Besra, C. M. J. E. Vandenbroucke-Grauls, W. Bitter and A. M. Sar, "Zebrafish embryo screen for mycobacterial genes involved in the initiation of granuloma formation reveals a newly identified ESX-1 component," Disease models & mechanisms, vol. 4, pp. 526-536, 2011.
[50] L. Ramakrishnan, "Revisiting the role of the granuloma in tuberculosis," Nature Reviews Immunology, vol. 12, p. 352, 2012.
[51] L. Ramakrishnan, "The zebrafish guide to tuberculosis immunity and treatment," in Cold Spring Harbor symposia on quantitative biology, 2013.
[52] C. L. Cosma, K. Klein, R. Kim, D. Beery and L. Ramakrishnan, "Mycobacterium marinum Erp is a virulence determinant required for cell wall integrity and intracellular survival," Infection and immunity, vol. 74, pp. 3125-3133, 2006.
[53] O. A. Brady, E. Jeong, J. A. Martina, M. Pirooznia, I. Tunc and R. Puertollano, "The transcription factors TFE3 and TFEB amplify p53 dependent transcriptional programs in response to DNA damage," ELife, vol. 7, p. e40856, 2018.
[54] J. A. Martina, H. I. Diab, O. A. Brady and R. Puertollano, "TFEB and TFE3 are novel components of the integrated stress response," The EMBO journal, vol. 35, pp. 479-495, 2016.
[55] A. Balasubramani, Lysosomal calcium in dendritic cell migration, American Association for the Advancement of Science, 2017.
[56] A. Sumoza-Toledo, I. Lange, H. Cortado, H. Bhagat, Y. Mori, A. Fleig, R. Penner and S. Partida-Sánchez, "Dendritic cell maturation and chemotaxis is regulated by TRPM2-mediated lysosomal Ca2+ release," The FASEB Journal, vol. 25, pp. 3529-3542, 2011.
[57] Y. Dou, H.-j. Wu, H.-q. Li, S. Qin, Y.-e. Wang, J. Li, H.-f. Lou, Z. Chen, X.-m. Li, Q.-m. Luo and others, "Microglial migration mediated by ATP-induced ATP release from lysosomes," Cell research, vol. 22, pp. 1022-1033, 2012.
[58] O. A. Brady, J. A. Martina and R. Puertollano, "Emerging roles for TFEB in the immune response and inflammation," Autophagy, vol. 14, pp. 181-189, 2018.
[59] D. Malhotra, J. Shin, L. Solnica-Krezel and E. Raz, "Spatio-temporal regulation of concurrent developmental processes by generic signaling downstream of chemokine receptors," eLife, vol. 7, p. e33574, 2018.